

On-beam synchrony in the cerebellum as the mechanism for the timing and coordination of movement

D. H. Heck*, W. T. Thach^{†‡}, and J. G. Keating[§]

*Department of Anatomy and Neurobiology, University of Tennessee Health Science Center, Memphis, TN 38103; †Departments of Anatomy and Neurobiology and Neurology, Washington University, St. Louis, MO 63110; and ‡Department of Neurology, University of Pennsylvania, Philadelphia, PA 19104

Edited by Edward G. Jones, University of California, Davis, CA, and approved March 5, 2007 (received for review November 14, 2006)

In trained reaching rats, we recorded simple spikes of pairs of Purkinje cells that, with respect to each other, were either aligned on a beam of shared parallel fibers or instead were located off beam. Rates of simple spike firing in both on-beam and off-beam Purkinje cell pairs commonly showed great variety in depth of modulation during reaching behavior. But with respect to timing, on-beam Purkinje cell pairs had simple spikes that were tightly time-locked to each other (either delayed or simultaneous) and to movement, despite the variability in rate. By contrast, off-beam Purkinje cell pairs had simple spikes that were not time-locked to each other, neither delayed nor simultaneous. We discuss the implications of these observations for the cerebellar role in timing and coordinating movement.

parallel fibers | Purkinje cell | simple spike | awake reaching rat

In the mammalian cerebellar cortex, excitatory and inhibitory neuronal processes run in exactly perpendicular directions. This network provides a common excitatory input to neurons along the mediolateral (parallel-fiber on-beam) axis and a common inhibitory input to neurons along the anterior-posterior (parallel-fiber off-beam) axis. The anisotropic network is highly preserved across vertebrate species and has been proposed to be the basis of cerebellar control of timing and coordination of movement. In the original proposals (1, 2), on-beam Purkinje cells (Pcs) were hypothesized to be activated one by one in a strict temporal sequence by a traveling wave of parallel-fiber activity, the rate and timing of which were determined by parallel-fiber conduction velocity. To test this hypothesis, we recorded with multiple electrodes the simple spike (SS) activity of pairs of Pcs in awake trained rats as they reached for, grasped, and returned a food pellet to the mouth. We found that on-beam pairs of Pcs generated two types of temporally correlated SS activity. In one type, there was a delay of the second SS with respect to the first that was proportionate to the parallel-fiber conduction velocity. However, this delayed correlation was observed rarely, was weak when present, and was poorly time-locked to movement. In the second type of on-beam SS correlation, the SSs of the Pc pairs occurred simultaneously with no delay and were precisely synchronized. This synchronous on-beam correlation was common (observed in SSs of almost all Pc pairs), was robust when present, and was precisely time-locked to movement. By contrast, the SSs of off-beam Pc pairs were not correlated with each other (neither delayed nor synchronous). We discuss the possibility that the observed Pc SS on-beam synchrony that is time-locked to movement may be the organizing principle for the cerebellar timing and coordination of movement.

Results

We recorded SS activity from the Pc layer of the cerebellar cortex of awake reaching rats (see Fig. 5 in *Materials and Methods*). SS activity in the paramedian lobe was strongly

modulated during performance of reaching and grasping movements (Fig. 1). We recorded simultaneously with three electrodes that were linearly aligned and spaced at 305 μm . Recording sites were thus separated by 305 or 610 μm . Because both the axons of the excitatory granule cells (parallel fibers) and those of the inhibitory neurons are of finite length, the amount of common input both on and off beam could be expected to decrease with distance (3). Therefore, we expected a fall off in common spike activity recorded across electrodes with increasing interelectrode distance. To see whether this expectation was the case, we performed a cross-correlation analysis on pairs of simultaneously recorded neurons.

On-Beam SS Temporal Correlation with Delay. Seemingly in agreement with original beam theory predictions (1, 2), our analysis revealed that some on-beam Pc pairs did indeed have a delayed temporal correlation. Occasionally, the correlated activity occurred at a delay that matched the estimated parallel-fiber conduction velocity 0.5 m/s (305 μm apart, +0.6 ms, $P = 0.0007$; -0.6 ms, $P = 0.00003$) (Fig. 2). A similar observation has been made in anesthetized cats (4). However, at the larger distance (610 μm), the delayed correlation at 1.2 ms was no longer significant. Further, the delayed correlation of spike activity was only weakly time-locked to movement. Delayed SS correlations during unsuccessful reaches were slightly higher than during successful reaches ($P = 0.0013$). Thus, although a traveling wave of parallel-fiber activity may conceivably affect Pc SS timing, this effect is only over short distances of $\approx 300 \mu\text{m}$, the occurrence is rare, the correlation is weak, and the time-locking to successful movement is poor.

On-Beam SS Simultaneous Synchronization. To our surprise, by far the biggest SS correlation of on-beam Pc pairs was simultaneous, occurring at zero delay. Pairs of on-beam Pcs fired simultaneous synchronized SSs during the reaching and grasping movement, and the occurrence was tightly time-locked to touching the food pellet reward. Synchrony between close (305 μm) and distant (610 μm) pairs was equally precise. We believe that this tight synchrony was not caused by electrical noise artifact for several reasons. (i) No such synchrony occurred between Pc pairs that were off-beam with respect to each other despite otherwise identical recording conditions. The difference between on- and off-beam zero-lag correlation was highly significant ($P =$

Author contributions: D.H.H. and W.T.T. designed research; D.H.H. and W.T.T. performed research; D.H.H. and J.G.K. analyzed data; and D.H.H., W.T.T., and J.G.K. wrote the paper.

The authors declare no conflict of interest.

This article is a PNAS Direct Submission.

Abbreviations: Pc, Purkinje cell; SS, simple spike.

[†]To whom correspondence should be addressed at: Washington University, 600 South Euclid Avenue, St. Louis, MO 63110. E-mail: thachw@pcg.wustl.edu.

© 2007 by The National Academy of Sciences of the USA

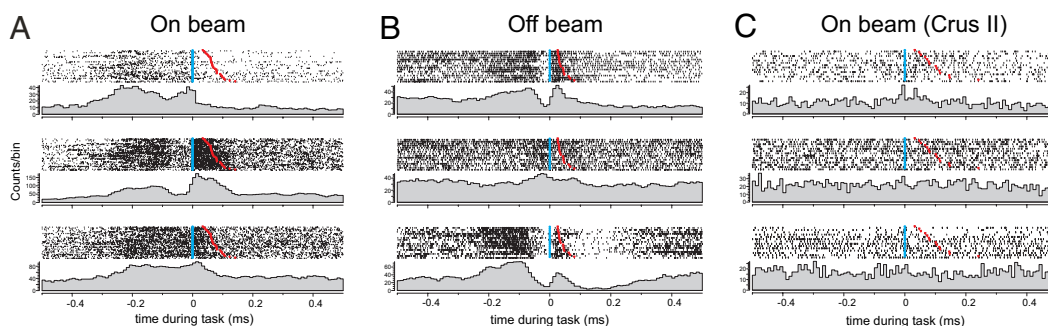


Fig. 1. Pc SS activity in the paramedian lobe is strongly modulated during reaching–grasping movements. On-beam and off-beam Pc SS activity was recorded with a linear array of three extracellular recording electrodes. Electrodes were inserted into the cerebellar cortex of head-fixed rats that were trained to use their preferred forepaw to reach for a small food pellet while under head fixation (30, 31). Recordings were performed in the ipsilateral paramedian lobe, which contains a forepaw representation area, with the electrode array either in on-beam or off-beam orientation. Electrodes were lowered to the Pc layer, and Pc I activity was identified by the presence of complex spikes (32). SSs and complex spikes were recorded and analyzed off-line (5). SS activity was analyzed in terms of firing rate and in terms of temporal correlations between recording sites (5). Reaching–grasping movements were videotaped and analyzed off-line. Successful and unsuccessful trials were analyzed separately. Blue dots indicate alignment of spike activity on the time the rat's paw first touched the food pellet. Red dots indicate the time the paw left the capacitance switch. (Top to Bottom) Peri-event time histograms of spike activity recorded on electrodes 1, 2, and 3. (A) Recording from the arm representing area of the paramedian lobe with the recording sites aligned with the direction of parallel fibers (on beam). (B) Recording from the same area of the paramedian lobe as in A with the recording sites aligned perpendicular to the direction of parallel fibers (off beam). (C) For control purposes, on-beam neuronal activity was also recorded in crus II (a non-arm-related area). As expected, neuronal activity in crus II Pcs did not change during the reaching and grasping behavior. Activity recorded in the paramedian lobe showed movement-related activity changes independent of the alignment of recording sites.

$1.9082e-10$) (Fig. 3B). (ii) On-beam recordings in crus II, an area close to the paramedian lobule not involved in arm movement, did not show such synchrony (Fig. 3C). (iii) In rare instances, on-beam Pc SS synchrony was absent. (iv) When it occurred, it was time-locked to the reach (Fig. 3A).

The method we used to investigate and quantify whether and how on-beam synchrony was related to the reaching and grasping behavior was that of time-resolved cross-correlation analysis (5). The results revealed that the on-beam synchronous activity was a common and highly statistically significant phenomenon. Of 32 Pc on-beam pairs that showed movement-related SS changes, 31 (97%) also showed epochs of significant synchronous activity during the movement. On-beam synchronous firing occurred preferentially during the extension phase of the reaching movement (Fig. 4). By contrast, changes in firing rates occurred during both the extension and retraction phase (see below).

Rates of Firing of On-Beam Pc SS Pairs Are Not Correlated. According to the original beam hypothesis, pairs of on-beam Pcs should have similar behavior-related SS rates. Off-beam neuronal pairs, on the other hand, should have different rates because they all receive different excitatory inputs. Surprisingly, on-beam behavior-related SS rates of Pc pairs were as highly varied and as poorly correlated with each other as were SS of off-beam Pc pairs [on-beam: mean correlation coefficient, 0.35 ± 0.35 ; range, 0.86 to -0.41 ; off-beam: mean correlation coefficient, 0.23 ± 0.32 ; range, 0.67 to -0.35 (ref. 5)]. Thus, rates of SSs of on-beam Pc pairs seemed to show no signs of common parallel-fiber input to Pcs, contrary to the prediction of the original beam hypothesis (1, 2).

Discussion

This work found that on-beam pairs of Pcs in the cerebellar cortex of awake behaving rats fire SSs that are precisely correlated in time in both of two ways: one simultaneous and synchronized (commonly and robustly), the other delayed (rarely and weakly). The interval timing of the delayed correlations matched the delays expected from activity traveling along the parallel fibers. Such correlations were not observed between neurons separated by $>300 \mu\text{m}$, indicating that traveling waves of parallel-fiber activity only affect Pc spike timing over short distances.

Behavior-related on-beam synchrony was commonly found (in 31 of 32 paired recordings) and therefore seems to be a rule of cerebellar network activity rather than an exception. Synchronized on-beam activity was tightly time-locked to certain phases of the movement. Importantly, changes in behavior-related SS rates and the occurrence of behavior-related on-beam synchrony were independent of each other. They thus seem to be related to different aspects of the movement and may represent independent control signals. Off-beam Pc SS neuronal pairs were not temporally correlated. Finally, the SSs of pairs of Pcs both on beam and off beam fired in rates that were highly varied and not correlated. Thus, there were no signs of common parallel-fiber inputs in the behavior-related on-beam activity as predicted by the beam hypothesis (2).

What Causes the On-Beam Synchrony? We were able to exclude climbing fiber inputs as a possible source for on-beam synchrony because the synchronized spikes were not associated with the occurrence of complex spikes. On-beam synchronous SS firing occurred with virtually zero lag time. The most plausible explanation is that such precise synchronization is caused by common input to the observed neurons. At any given site in the cerebellar granular layer, several mossy-fiber termination fields overlap, providing combined sources of common input. Mossy fibers branch out extensively in the granule cell layer and form large numbers of complex synaptic terminals (glomeruli) (6), each of which contacts several granule cells, and each granule cell receives input from approximately seven different mossy fibers (7). A single mossy fiber will thus provide common excitatory inputs to a large number of granule cells that, in turn, will provide synchronous excitatory inputs to Pcs and inhibitory interneurons. It must be assumed that the common mossy-fiber input is transmitted to Pcs by the short ascending axons of granule cells because any parallel-fiber involvement would cause delays proportional to on-beam distance. The movement related on-beam synchrony could thus reflect epochs of temporal correlations between mossy-fiber inputs.

The lack of synchronous activity between off-beam pairs of Pcs, on the other hand, may be caused by the activity of inhibitory interneurons (basket and stellate cells) that receive the same mossy-fiber inputs and have axons projecting exclusively in off-beam direction. Basket and stellate cells will therefore

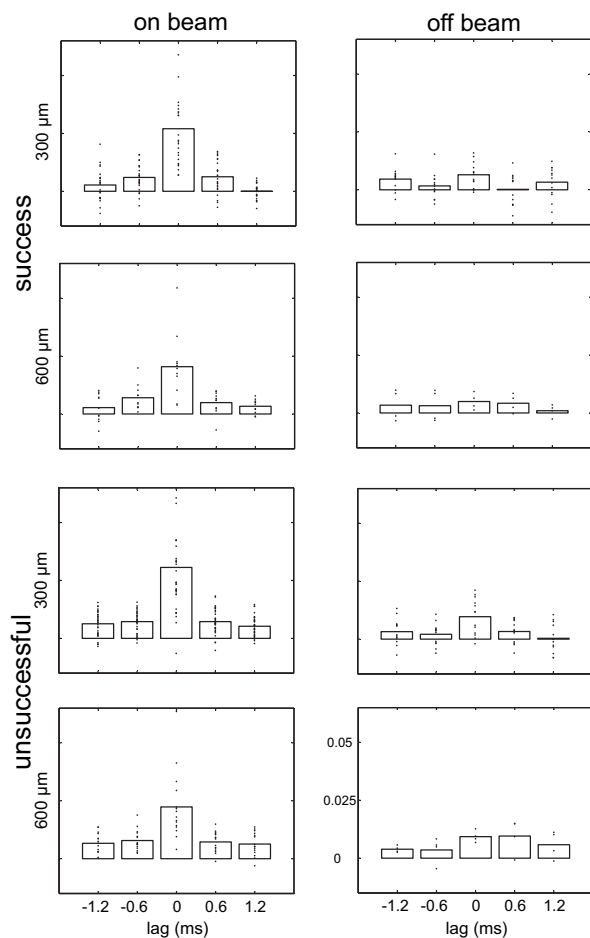


Fig. 2. Precise temporal correlation of SS activity between on-beam but not off-beam pairs of neurons. We tested for significant differences in temporal correlations of SS activity in paired on-beam and off-beam recordings by using the Wilcoxon rank sum test. On-beam pairs of Pcs showed a significantly higher correlation than off-beam pairs at 0.6 ms, i.e., a delay that matched the parallel-fiber conduction velocity (+0.6 ms, $P = 0.0007$; -0.6 ms, $P = 0.00003$). However, the delayed correlation at 1.2 ms between distant neighbors (610 μm) was no longer significantly different between on- and off-beam pairs of Pcs (+1.2 ms, $P = 0.060$; -1.2 ms, $P = 0.067$). Each plot is centered on "0 delay," i.e., the synchronous occurrence of SS events. The temporal delay predicted by parallel-fiber conduction delay depends on the distance between recording sites. Predicted delays (based on a parallel-fiber conduction velocity of 0.5 m/s) were 0.6 and 1.2 ms for electrodes separated by 305 and 610 μm , respectively. The side bars are centered on the temporal intervals predicted by the parallel-fiber delays. Each plot shows the excess correlation coefficient (after subtraction of the shift predictor) for the period 500 ms before and after the paw touched the food pellet. Bars show the excess correlation, and each point reflects the data from a single paired recording. Data from all paired recordings are shown. Correlation of on-beam spike activity was significantly higher than that of off-beam activity at 0.6-ms delay and at zero lag, i.e., synchronous activity.

generate off-beam inhibition that is synchronized with the common mossy-fiber input. Thus, on-beam synchrony is likely the result of common mossy-fiber inputs transmitted to a large number of Pcs by ascending granule cell axons, and the lack of off-beam inhibition may be caused by the synchronized lateral inhibition through basket and stellate cells. This mechanism would also explain the correlation between on-beam synchronous firing and certain phases of the behavior because epochs of on-beam synchrony would reflect epochs of behavior-related increases in mossy-fiber activity.

What Is the Result of the On-Beam Synchronicity? Previously (8) we had remarked how in the macaque the parallel fibers in the

cerebellar cortex run more or less parallel to the myotomes of the body maps in the deep nuclei (9, 10). We speculated that the parallel-fiber beam may thus through Pc inhibition modulate coordination of the natural myomeric synergists mapped within the deep nuclei. In addition, parallel fibers would be long enough to span (by Pc projections) two or more adjacent nuclei, fastigius controlling stance and gait, interpositus agonist/antagonist coordination at a single joint, and dentate eye-limb coordination in reaching and of digits in multidigit movements. Bastian *et al.* (11) reported how this theory might explain the inability to coordinate bilateral body movements in gait and balance after vermal section in humans. The studies of Cicirata *et al.* (12, 13) show that there is similar somatotopic organization in the deep cerebellar nuclei of the rat, at least for head and forelimb. Further studies to pursue this reasoning might consist of on- and off-beam Pc recording as described here combined with electromyographic recording of synergists and antagonist muscles and the time of activation and magnitude/rate of activation.

Variation of SS Rates of Pcs Along the Parallel-Fiber Beam. The variability of the on-beam spike rates can perhaps be explained by the powerful inputs from the ascending parts of the granule cell axons, which provide each Pc with inputs from a different subset of granule cells (14). Alternatively, each Pc could only receive functional inputs from a small subset of parallel fibers, with every cell responding to a different subset (15). Two recent studies strongly support the view that individualized parallel-fiber input provides every Pc with unique response properties. Isope and Barbour (16) reported that a majority of parallel-fiber to Pc synaptic contacts were "silent," i.e., they produced no detectable postsynaptic effect. Jorntell and Ekerot (17) demonstrated that Pcs in rats responded only to a small fraction of the sensory information available to them through their parallel-fiber inputs. The authors suggested that the suppression of receptive fields was caused by a down-regulation of parallel-fiber inputs by long-term depression (18). Evidence presented here and in the two above-cited studies thus indicate that on-beam Pcs receive highly individualized, independent parallel-fiber inputs. These findings could settle a long-standing debate about whether parallel fibers control Pc spike activity or have subthreshold modulatory function (14, 19, 20). Our findings together with those of Isope, Jorntell, and their respective colleagues indicate that the response properties of each Pc are shaped by only a small selected subset of the $\approx 170,000$ parallel-fiber inputs they receive (21) and that no two Pcs respond to the same subset of inputs. As a result, on-beam Pcs receive input from different groups of parallel fibers carrying different types of information. Consequently, different Pcs have different response properties. Our data show that the interindividual differences between the response properties of on-beam Pcs are just as large as the differences between off-beam Pcs. Another consequence of this input-selection mechanism is that activity traveling along the parallel fibers cannot be expected to trigger sequential spiking in neighboring cells, which explains why on-beam Pc activity does not reflect parallel-fiber activity spreading along the beam as proposed by Eccles *et al.* (2).

Our findings thus support a revised version of the beam hypothesis of cerebellar function presented by Braitenberg (1) and by Eccles *et al.* (2). The original beam hypothesis suggested that the orthogonal arrangement of excitation and inhibition in the cerebellar network would result in high levels of Pc SS activity along a beam of parallel fibers, with lateral inhibition by basket and stellate cells suppressing Pc activity in flanking parallel beams. But, based on firing rates, no signs of lateral inhibition or elevated on-beam excitation were found, although this work does not rule out such influences. Time-resolved correlation analysis of behavior-related spike activity, however, revealed an intriguing aspect of cerebellar network activity that

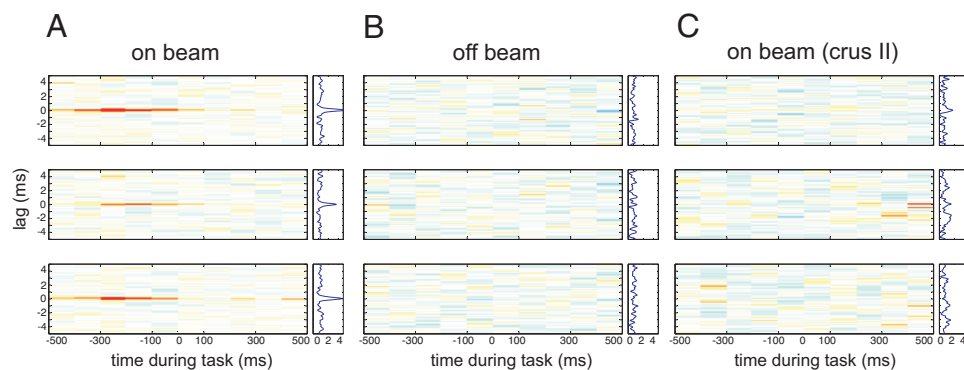


Fig. 3. On-beam Pcs in the paramedian lobe fired precisely synchronized SSs time-locked to behavior. Each plot represents the time-resolved cross-correlogram of Pc SS activity recorded at two different electrodes during reaching–grasping movements. Average cross-correlations were calculated for epochs of 100-ms duration with a temporal resolution of spike delays of 40 μ s. In each plot, the abscissa indicates time during the movement. At time 0, the rat has completed paw extension and touches the food pellet. The ordinate indicates the cross-spike train interval. All plots use the same color map (from red = 0.01 through white = 0 to blue = -0.01). Plots to the right side of the time-resolved cross-correlation matrix show the average excess correlation, i.e., the integral along the abscissa. The time-resolved cross-correlations shown here were generated from the same data shown in Fig. 1. Data were analyzed by subdividing the experimental time into 100-ms bins and calculating the average excess correlation within each bin at 40- μ s resolution. The resulting color-coded matrix was smoothed across delays by convolving with a 120- μ s Gaussian. (A) Correlation analysis of spike activity recorded with the electrode array in on-beam orientation in the paramedian lobe. (Top to Bottom) Plotted cross-correlations of spike activity recorded on electrode 1 versus 2, 2 versus 3, and 1 versus 3. Behavior-related occurrence of on-beam synchronous activity is visualized by the red lines at zero lag in the on-beam matrix. The occurrence of synchronous activity was not directly correlated with spike rate or change of rate. (Middle) Time-resolved cross-correlation of the spike activity shown in Fig. 1A Middle and Bottom. The peristimulus time histogram in Fig. 1A show that neurons at both recording sites reach their maximum firing rate shortly after the animal grabbed the pellet (i.e., after time 0) but that this time is not maximum excess correlation. Excess correlation is maximal at -200 to -100 ms, a period where the rate is relatively constant at an intermediate level. Thus, the temporal correlation and the rate of SS activity of pairs of on-beam Pcs change independently. (B Top to Bottom) Arrangement of cross-correlation plots as in A. Here, the electrode array was in off-beam orientation. No synchronous activity was seen in paired off-beam recordings. (C) Correlation analysis of SS activity recorded during behavior in crus II, an area outside the arm representation, with the electrode array in on-beam orientation. No behavior-modulated SS activity or synchronous firing was observed.

provides a possible link among the structure of the cerebellar network, its neuronal activity, and cerebellar control of behavior.

Many questions about the behavioral significance of the cerebellar network architecture remain open. For example, it is still unclear how much excitatory parallel-fiber inputs and inhibitory inputs from interneurons contribute to shaping behavior-related Pc activity. The on- and off-beam spatial relationships do not determine behavior-related changes in SS rates but rather determine whether or not two Pcs are likely to be synchronously active during behavior. It is conceivable that synchrony of SS activity of pairs of Pcs separated along a parallel-fiber beam determines which motor neurons and muscles will be linked in multijointed, multimuscled movement temporospatially coordinated movement. By contrast, the variation in firing rates of the SS pairs linking muscles in a coordinative unit may determine the varying tension with which those muscles must act to serve their respective roles in the movement. Such a mechanism that deals with each of muscle timing, selection, and tension could be tested by correlating the SS firing timing and rates with those of the electromyograph of muscles they may control, which could possibly reconcile the issues on cerebellar timing versus coordination of movement (22–24).

Materials and Methods

All animal procedures performed during in this work were in accordance with institutional guidelines at the Washington University in St. Louis. Sprague–Dawley rats (2–4 months old) were trained to perform a reaching–grasping task with their right forepaw. After learning, animals underwent surgery during which the skull over crus II of the ipsilateral cerebellum was removed, and a capped recording chamber was mounted over the opening. Two upside-down machine screws were mounted on the head, allowing the animal's head to be immobilized during the electrophysiological recording sessions. Four skull screws were inserted into the skull to serve as anchors for the acrylic cement that was poured around the recording chamber and the

head fixation screws (Fig. 5A). After recovering from surgery, animals were retrained to reach for pellets under head-fixed conditions (Fig. 5B). The behavioral performance was taped on video and later used to classify reaches into successful or unsuccessful, with or without correction movements. Touching of the food pellet set off a capacitance switch that triggered a transistor–transistor logic (TTL) pulse and turned on a light-emitting diode (LED) light (blue dots in Fig. 1). The TTL signal was recorded in the same data file as the spike data to allow off-line event-triggered analysis. The LED light signal indicated capacitance switch activation in the video recordings and was used for temporal alignment of reaching events recorded on video with TTL signals recorded in the data files. Time of withdrawal of the paw from the capacitance switch after grasping the food pellet was also recorded and stored (red dots in Fig. 1).

Analysis was restricted to reaching–grasping movements that were performed as a single, smooth forepaw extension–retraction movement. Those were subdivided into successful (if the pellet was grabbed) and unsuccessful reaches (if the pellet was missed). Unsuccessful reaches analyzed here were completed like successful ones in that the animal would bring the paw all of the way back to the mouth. Trials during which the rats made correction movements trying to retrieve an initially missed pellet were excluded from analysis.

Multiple-electrode recordings of task-related Pc SS activity were performed by using a linear array of three electrodes. Electrodes were either aligned with the direction of parallel fibers or perpendicular to the parallel fibers. The correct alignment with the parallel fibers was determined by electrical stimulation with one electrode and successful recording of parallel-fiber population spike responses on the other two. The alignment procedure was performed in crus II. As the electrodes were lowered to the paramedian lobe, slight deviations between electrode array orientation and parallel fibers could have occurred. For recordings perpendicular to the parallel fibers, the electrode array was rotated 90°.

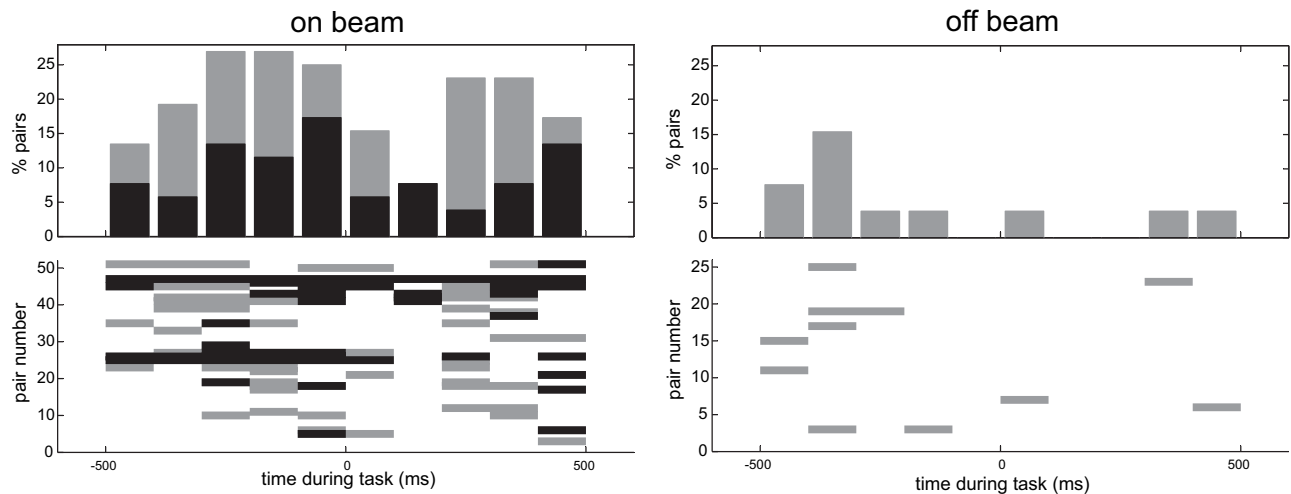


Fig. 4. On-beam synchronous Pc SS activity occurs preferentially during the extension phase of the reaching movement. Time during the task (experimental time) was subdivided into bins of 100-ms duration (for details, see *Materials and Methods*). For each paired recording, the zero lag correlation within these bins was calculated and compared with baseline correlation. Bins with excess correlation >3 SD of the baseline are colored black. Those between 2 and 3 SD are colored gray. (Left) On-beam synchronous firing occurred mostly during a period of 300 ms before the rat touched the pellet followed by a sudden drop in synchronous activity right at the time of the grasp (at 0 ms). Hence, synchronous firing was most frequent during the extension phase of the reaching movement. (Right) Off-beam synchrony never exceeded the 3 SD level and did not show temporal modulation with the movement. The time-resolved cross-correlations were calculated by using 40- μ s bins. Baseline correlation was obtained by calculating the mean \pm SD of the correlation values at ± 1.8 -ms delay.

Multiunit activity was recorded from the Pc layer [as determined by the presence of complex spikes (25)] in the ipsilateral paramedian lobe or crus II. We used a multiple-electrode recording system that allowed adjusting the depth of each electrode individually (System Eckhorn; Uwe Thomas Recording, Giessen, Germany). Electrode depth could be adjusted with micrometer resolution and was displayed on a computer monitor. Interelectrode spacing was 305 μ m. Electrodes were made out of glass-coated tungsten–platinum alloy with an outer diameter of 80 μ m and impedances of 1–5 MOhm. The electrodes were lowered individually into the same Pc layer, and the rat was allowed to reach. Electrode signals were bandpass-filtered (0.1 Hz to 8 kHz) and digitized continuously at sampling rates above 20 kHz per channel (CED, Cambridge, U.K.). Raw data were

stored on a hard disk and digitally high-pass-filtered at a cutoff frequency of 300 Hz before off-line analysis of spike activity (Spike2; CED). SSs were detected after filtering by using a fixed threshold of 3 SD of baseline noise.

Data Analysis. We used a noise reduction technique to remove common activity across electrodes and to improve our signal-

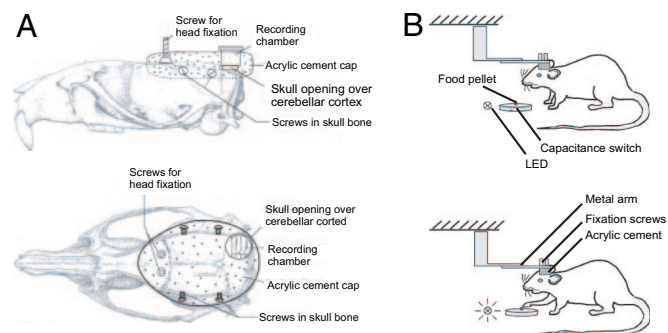


Fig. 5. Schematic illustration of head holder, recording chamber design, and experimental procedure. (A) Schematic illustration of how head fixation screws, skull screws, and the recording chamber were mounted on the rat's head. All parts were embedded in acrylic cement (Co-ral-lite Dental Mfg. Co., Diamond Springs, CA). (B) Schematic illustration of a rat in the head fixation device with the capacitance switch and the food pellet in front. Individual food pellets were presented on the capacitance switch carefully placed in the same spot each time. The paw touching the food pellet, i.e., coming close to the capacitance switch, set off the switch, which was recorded in the data file (TTL pulse) and on video (LED light). Reach training under head fixation started at 3–5 days after surgery. It took between 2 and 3 days for the rats to learn to reach for pellets with their heads fixed.

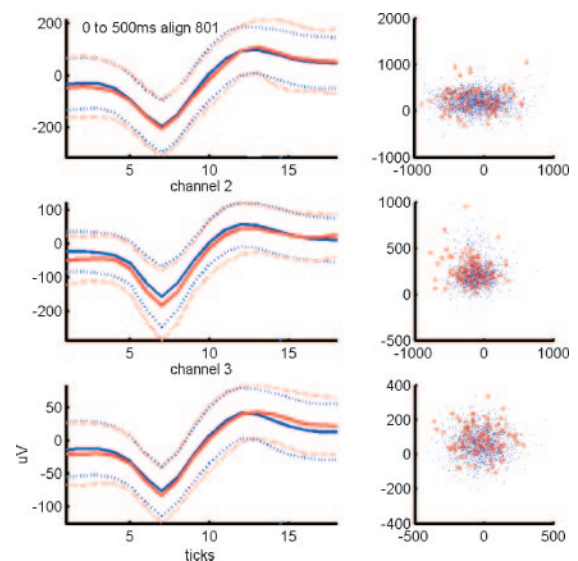


Fig. 6. Principal-component analysis of the waveform shapes of synchronized and nonsynchronized spikes reveals that synchronized events are spikes, not artifacts. To ensure that the occurrence of synchronous spikes with millisecond precision were not caused by technical artifacts, we compared the shapes (Left) and principal components (Right) of spikes that had a synchronous partner on one or both of the other channels (red lines, respective dots) with nonsynchronized spikes (blue lines, respective dots). This comparison revealed no difference between the two populations, indicating that synchronous events were indeed spikes and not artifacts, e.g., caused by capacitive coupling between channels. Synchronized spikes were not associated with the occurrence of complex spikes.

to-noise ratio (26). Spikes were detected by using a threshold defined by 3 SD of the signal. All data analysis presented here was performed on multiunit signals.

Cross-correlation analysis and shift-predictor correction. Average cross-correlations. Average cross-correlations of on-beam spike activity were calculated to determine whether on-beam neurons are activated sequentially by traveling parallel-fiber activity. Parallel fibers conduct action potentials at a velocity of ≈ 0.5 m/s (rat) (27). With distances between recording sites of 305 or 610 μm , the expected parallel-fiber conduction delays were ≈ 0.6 and ≈ 1.2 ms, respectively. We cross-correlated spike activity from all adjacent (305 μm) and distant (610 μm) pairs, by using 0.6-ms-wide bins centered at 0.0 ± 0.6 and ± 1.2 ms. The data shown in Fig. 2 of the manuscript are “excess correlations,” i.e., the raw correlations minus the expected correlations caused by variation in rate. Synchronized action potentials and action potentials with a certain delay will inevitably occur by chance. When firing rates increase, the chances of two spikes occurring at the same time or with a specific delay also increase. The number of these chance events can be estimated by calculating the “shift predictor” (28), which is a histogram of the expected “by chance” correlations between two spike trains. The shift predictor is subtracted from the raw correlation to reveal the “above chance” or excess correlation.

The shift predictor was calculated by cutting the spike trains into pieces of single trial length and recording correlating spikes during different trials. For example, the response of neuron 1 in trial 1 will be correlated with the response of neuron 2 in trials 2– n . Ideally, correlations for all possible shifts of trials would be calculated and averaged to yield the best possible shift predictor, which is mathematically equivalent to calculating the cross-correlation of the peri-event time histograms of the two neurons (28), as we did in this work. The resulting shift predictor is then subtracted bin by bin from the raw correlation to yield excess correlation.

“Time-resolved” cross-correlations. The standard average cross-correlation is typically calculated by using the data from the entire duration of the experiment. It provides information about the average magnitude and the delay of a correlation between two trains of events but cannot be used to detect changes of such a correlation during the course of the experiment. The time-resolved cross-correlation provides information about when correlated events occurred, which is achieved by calculating standard average cross-correlations for successive short intervals of experimental time. The time-resolved cross-correlation analysis thus produces a number of standard correlation histograms, each representing the average correlation of events during a brief

epoch of the experimental time. If the correlation of events changes over time, as was the case with the on-beam synchronous firing reported here, time-resolved cross-correlation will reveal these changes. Time-resolved cross-correlations were calculated from multiunit spike trains to determine the dynamic changes of excess correlation in spike activity during behavior. To this end, average cross-correlations were calculated for brief epochs of 100-ms duration with a temporal resolution of spike delays of 40 μs . For each 100-ms epoch, excess correlations, i.e., those exceeding expectation based on the firing rates of the two neurons, were calculated by subtracting the shift predictor from the raw correlation. The results from all 100-ms epochs were color-coded and plotted in form of a color-coded matrix with experimental time plotted on the x axis and spike delay on the y axis (Fig. 3).

Analyzing 5Ss responsible for on-beam synchronous activity. Synchronous spike activity at submillisecond precision could raise concerns about the possibility that the finding may be artifactual. Synchronous Pc activity with the same, astonishing temporal precision was observed with different recording equipment and in a different animal (cat) under anesthesia (4, 29). Such synchrony could conceivably be the result of a misinterpretation of electrical artifacts. Such artifacts typically occur on all recording channels simultaneously and could be mistaken for action potentials. The shapes of these artifacts, however, are usually very different from the shapes of action potentials. We therefore analyzed the shapes of the action potentials that were part of on-beam synchronous activity and compared them with the shapes of nonsynchronized spikes. Principal-component analysis of spike shapes revealed that synchronized and nonsynchronized spikes had identical shapes, making it unlikely that nonneural electrical artifacts were wrongly interpreted as action potentials (Fig. 6). Furthermore, should technical artifacts have occurred, it would be difficult to explain why they occurred exclusively during on-beam recordings in the paramedian lobe. If the orientation of the electrode array had anything to do with catching an artifactual signal, on-beam recordings from crus II, which we performed as a control experiment, should have revealed synchronous activity but did not. We therefore conclude that the behavior-related on-beam synchrony reported here is a genuine neuronal activity pattern of the cerebellum.

New analyses were performed from previously recorded and reported data (30). We thank Ruth Clark for help with animal training, reach classification, and recording, and Matthew Ennis for comments on earlier versions of the manuscript. This project was supported by National Institutes of Health Grant NS R01-1777 and a McDonnell grant (to W.T.T.) and a DFG Fellowship (to D.H.).

- Braitenberg V (1961) *Nature* 190:539–540.
- Eccles JC, Ito M, Szentágothai J (1967) *The Cerebellum as a Neuronal Machine* (Springer, Berlin).
- Heck DH (1999) *Neurosci Lett* 263:137–140.
- Bell CC, Grimm RJ (1969) *J Neurophysiol* 32:1044–1055.
- Baker SN, Spinks R, Jackson A, Lemon RN (2001) *J Neurophysiol* 85:869–885.
- Palay SL, Chan-Palay V (1974) *Cerebellar Cortex: Cytology and Organization* (Springer, Berlin).
- Llinás R (1982) in *The Cerebellum, New Vistas*, eds Palay SL, Chan-Palay V (Springer, New York), pp 189–192.
- Thach WT, Goodkin HP, Keating JG (1992) *Annu Rev Neurosci* 15:403–442.
- Thach WT, Jones EG (1979) *Brain Res* 169:168–172.
- Asanuma C, Thach WR, Jones EG (1983) *Brain Res* 286:267–297.
- Bastian AJ, Mink JW, Kaufman BA, Thach WT (1998) *Ann Neurol* 44:601–610.
- Cicirata F, Angaut P, Pantó MR, Serapide MF (1989) *Brain Res Rev* 14:117–141.
- Cicirata F, Angaut P, Serapide MF, Panto MR, Nicotra G (1992) *Exp Brain Res* 89:352–362.
- Wu HS, Sugihara I, Shinoda Y (1999) *J Comp Neurol* 411:97–118.
- Marr D (1969) *J Physiol (London)* 202:437–470.
- Isope P, Barbour B (2002) *J Neurosci* 22:9668–9678.
- Jornell H, Ekerot CF (2002) *Neuron* 34:797–806.
- Ito M (2001) *Physiol Rev* 81:1143–1195.
- Bower JM (2002) *Ann NY Acad Sci* 978:135–155.
- Garwicz M, Andersson G (1992) *Exp Brain Res* 88:615–622.
- Napper RMA, Harvey RJ (1988) *J Comp Neurol* 274:168–177.
- Hore J, Timmann D, Watts S (2002) *Ann NY Acad Sci* 978:1–15.
- Ivry R, Spencer RM, Zelaznik HN, Diedrichsen J (2002) *Ann NY Acad Sci* 978:302–317.
- Diener HC, Dichgans J, Guschlbauer B, Bacher M, Rapp H, Klockgether T (1992) *Mov Disord* 7:14–22.
- Thach WT (1970) *J Neurophysiol* 33:537–547.
- Musial PG, Baker SN, Gerstein GL, King EA, Keating JG (2002) *J Neurosci Methods* 115:29–43.
- Heck DH (1993) *Neurosci Lett* 157:95–98.
- Perkel DH, Gerstein GL, Moore GP (1967) *Biophys J* 7:419–440.
- Ebner TJ, Bloedel JR (1981) *J Neurophysiol* 45:948–961.
- Heck DH, Kuemmel F, Thach WT, Aertsen A (2002) *Ann NY Acad Sci* 978:156–163.
- Whishaw IQ, Pellis SM (1990) *Behav Brain Res* 41:49–59.
- Thach WT (1968) *J Neurophysiol* 31:785–797.